VIP Induces Changes in the F-/G-Actin Ratio of Schlemm's Canal Endothelium via LRRK2 Transcriptional Regulation

Xiaoqin Yan,[1] Mu Li,[1,2] Zhaoxia Luo,[1] Yin Zhao,[1] Hong Zhang,[1] and Liwen Chen[1]

[1]Department of Ophthalmology, Tongji Hospital, Tongji Medical College, Huazhong University of Science and Technology, Wuhan, China
[2]Department of Ophthalmology, Union Hospital, Tongji Medical College, Huazhong University of Science and Technology, Wuhan, China

Correspondence: Hong Zhang, Department of Ophthalmology, Tongji Hospital, Tongji Medical College, Huazhong University of Science and Technology, No. 1095 Jiefang Avenue, Qiaokou District, Wuhan, Hubei 430030, China; dr_zhanghong@vip.163.com. Liwen Chen, Department of Ophthalmology, Tongji Hospital, Tongji Medical College, Huazhong University of Science and Technology, No. 1095 Jiefang Avenue, Qiaokou District, Wuhan, Hubei 430030, China; dollychen69@gmail.com.

XY and ML contributed equally to the work presented here and should therefore be regarded as equivalent authors.

Received: September 12, 2019
Accepted: March 17, 2020
Published: June 22, 2020

Citation: Yan X, Li M, Luo Z, Zhao Y, Zhang H, Chen L. VIP induces changes in the F-/G-actin ratio of Schlemm's canal endothelium via LRRK2 transcriptional regulation. *Invest Ophthalmol Vis Sci.* 2020;61(6):45. https://doi.org/10.1167/iovs.61.6.45

Purpose. A previous study reported that vasoactive intestinal peptide (VIP) can regulate the cytoskeleton of Schlemm's canal (SC) endothelium and expand the SC lumen in a rat glaucoma model. In this study, we aimed to investigate the molecular mechanism of VIP on cytoskeleton regulation.

Methods. During in vivo experiments in rats, leucine-rich repeat kinase 2 (LRRK2) expression and the ratio of F-actin to G-actin (F-/G-actin) surrounding SC were examined by immunofluorescence after the application of VIP. For in vitro experiments in human umbilical vein endothelial cells, both quantitative PCR (qPCR) and western blotting were performed to evaluate Sp1 and LRRK2 expression after the application of VIP (and Sp1/LRRK2 inhibitor). In addition, the F-/G-actin ratio was examined by both immunofluorescence and western blotting after the application of VIP (and LRRK2 inhibitor).

Results. VIP induced increases in the expression of LRRK2 both in vivo and in vitro and the nuclear translocation of Sp1 in vitro. The application of Sp1 inhibitor abolished the increase in LRRK2 expression induced by VIP in vitro. In addition, VIP changed the F-/G-actin ratio, and this effect was abolished by the LRRK2 inhibitor both in vivo and in vitro.

Conclusions. VIP increased the expression of LRRK2, and this regulation was due to the nuclear translocation of Sp1. VIP further changed the F-/G-actin ratio and regulated the balance between the stabilization and destabilization of the F-actin architecture. This study elucidates a novel mechanism by which VIP regulates the actin cytoskeleton of SC endothelium via the Sp1–LRRK2 pathway, suggesting a potential novel treatment strategy for glaucoma.

Keywords: Schlemm's canal, vasoactive intestinal peptide, actin, leucine-rich repeat kinase 2, Sp1

Glaucoma is the leading cause of irreversible blindness worldwide,[1,2] and it is widely accepted that obstruction of the aqueous humor outflow pathway leads to an increase in intraocular pressure (IOP). The elevated IOP is considered to be the main risk factor for glaucoma. Lowering IOP is thought to be the only effective way to control the progression of glaucomatous retinal ganglion cell degeneration.[3,4] The dynamic balance between the generation and outflow of aqueous humor maintains IOP within normal.

The dysregulation of conventional outflow resistance can lead to a decrease in aqueous humor outflow and an increase in IOP, finally leading to the progression of glaucoma.[5] However, most of the current IOP-lowering pharmacological treatments are not aimed at the conventional outflow pathway, but rather at an unconventional outflow pathway or the generation of aqueous humor. Although these treatments have proven to be effective, they also have a range of side effects.[6,7] In addition, these anti-glaucoma treatments could also result in a consequent deprivation of aqueous humor passing the conventional pathway, causing further damage of the glaucomatous trabecular meshwork (TM) and Schlemm's canal (SC).[8,9] In terms of IOP-lowering treatments involving the conventional outflow pathway, most of them are destructive, including laser treatment of the TM or surgical removal or bypass of the TM and SC.[5] For this reason, new drugs targeting the conventional outflow pathway have been studied in recent years.[5,10–12]

In 1977, Kaufman et al.[13] found that by depolymerizing actin the aqueous humor outflow resistance can be reversibly reduced. After that, numerous other studies also showed that changes in the cytoskeleton can have an influence on aqueous humor outflow resistance, suggesting a possible role of the cytoskeleton in aqueous humor outflow resistance regulation.[14–17] These studies marked the

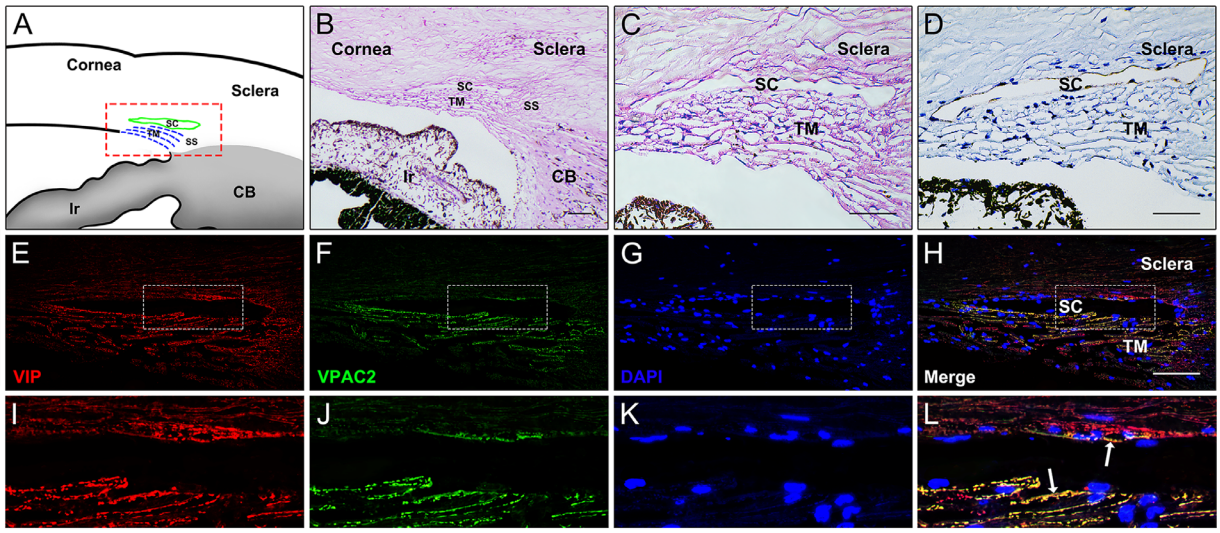

M

ID	Age	Sex	Eye	Cause of Death
1	49	Male	Right	Esophagus Cancer
2	35	Male	Right	Psychosis
3	67	Female	Right	Laryngocarcinoma
4	65	Female	Right	Liver Failure
5	62	Male	Right	Respiratory Failure
6	64	Male	Right	Pancreatic Cancer

Figure 1. Co-expression of VIP and VPAC2 in the region surrounding human SC. (**A**) Schematic diagram of anterior chamber angle. (**B**, **C**) Representative HE staining of SC (**B**, 20×; **C**, 40×). (**D**) Representative immunohistochemical (CD31) staining of SC (40×). Representative single staining of VIP (**E**, **I**), VPAC2 (**F**, **J**), and DAPI (**G**, **K**) in the region surrounding SC. (**H**, **L**) The merged figures show that VIP and VPAC2 were co-expressed in the region surrounding SC. (**M**) Characteristics of donors eyes. *Scale bars*: 50 µm.

beginning of investigations focusing on the relationship between the cytoskeleton and aqueous humor outflow.[18] Decreased outflow resistance can be attributed to increases in the density of SC inner wall pores and the separation of SC cells.[19] The depolymerization of actin can lead to a decrease in SC cell stiffness,[20] and less stiff SC cells are able to form more pores, thus decreasing the funneling effect and outflow resistance.[18,21] In addition, changes in the SC cell cytoskeleton can also result in changes in focal adhesions, thus affecting the attachment between SC and juxtacanalicular tissue, enlarging the spaces in the juxtacanalicular tissue and decreasing the funneling effect.[22,23] In contrast, the polymerization of actin can lead to increases in SC cell stiffness and aqueous humor outflow resistance, thus elevating IOP.[24–26] Our previous study[27] found that, vasoactive intestinal peptide (VIP) can regulate F-action distribution in the SC endothelium and thus expand the SC lumen and decrease IOP in a rat glaucoma model. Moreover, using human umbilical vein endothelial cells (HUVECs), we also found that VIP can change the ratio of F-actin to G-actin (F-/G-actin), which is closely related to the cell stiffness.[24,25] However, although the effect of VIP on the actin cytoskeleton of endothelial cells was identified, the mechanism remains unclear.

The *leucine-rich repeat kinase 2* (*LRRK2*) gene contains 51 exons and encodes a large, multidomain protein. The LRRK2 protein contains a couple of distinctive structural domains, including a Ras of complex proteins (ROC)/GTPase domain and a kinase domain.[28,29] In terms of its relationship with actin, previous studies have reported that the biological function of LRRK2 can be linked to the actin cytoskeleton and its dynamic regulation, indicating that LRRK2 possesses at least a basal regulatory activity on actin polymerization as a direct modulator.[30–32] One of the mechanisms by which LRRK2 regulates the actin cytoskeleton is its interaction with the small GTPases CDC42 and Rac1 (both of which are key regulators of actin polymerization)[31,33]; ezrin, radixin, and moesin (which are actin-binding proteins)[34]; and other actin stability- and maintenance-related proteins.[32] As a transcription factor, Sp1 can activate numerous molecular pathways, and its binding sequence is (G/T)GGGCGG(G/A)(G/A)(C/T),[35,36] which is also found in the LRRK2 promoter. Thus, Sp1 can bind to the LRRK2 promoter and promote LRRK2 expression.

In this study, we investigated the molecular pathway underlying the effects of VIP on the actin cytoskeleton and found that VIP regulates the F-/G-actin ratio via LRRK2, which is further regulated by the transcription factor Sp1.

Methods

Hematoxylin–Eosin Staining, Immunohistochemistry, and Immunofluorescence of Human SC Ex Vivo

We evaluated six normal donor eyes from the Department of Ophthalmology, Wuhan Red Cross Medical Center, Hubei, China. This study was approved by the ethics committee of Tongji Hospital and adhered to the tenets of the Declaration of Helsinki. A summary of the donor characteristics is provided in Figure 1. All obtained donor eyes were fixed in the 10% formalin at 4°C for 48 hours, and then each specimen from the donor eyes was divided into four sections,

which were subsequently embedded in paraffin to enable the SC to be cut perpendicular to its longitudinal axis.

For hematoxylin–eosin (HE) staining, the SC sections of hydrated and deparaffinized tissues were stained with hematoxylin and eosin following the standard protocols of histological observation.[37] For immunohistochemistry and immunofluorescence, SC sections (5 µm) were gently washed three times using PBS and were then treated with 10% donkey serum albumin for 1 hour at room temperature to block nonspecific bindings. For immunohistochemical staining, the sections were incubated overnight at 4°C with primary antibodies CD31/PECAM1 (1:100 dilutions; Cell Signaling Technology, Danvers, MA, USA). They were then washed with PBS and incubated with biotinylated secondary antibody. Then, 3′,3′-diaminobenzidine (DakoCytomation, Carpinteria, CA, USA) was used as the peroxidase substrate to develop a brown color, and hematoxylin (Merck Taiwan Ltd., Taipei City, Taiwan) was used as a counterstain. The immunohistochemical sections were observed by light microscopy. For immunofluorescence, primary antibody combinations of VIP (SC-25347, 1:200 dilution; Santa Cruz Biotechnology, Dallas, TX, USA) and vasoactive intestinal peptide receptors 2 (VPAC2) (AB2266, 1:100 dilution; MilliporeSigma, Temecula, CA, USA) were employed at 4°C overnight. After incubation of primary antibodies, the sections were washed with PBS and then incubated for 1 hour at room temperature with fluorescently labeled secondary antibodies: Alexa Fluor 594-conjugated donkey anti-mouse and Alexa Fluor 488-conjugated donkey anti-rabbit (1:200 dilutions; Thermo Fisher Scientific, Waltham, MA, USA) and 4′,6-diamidino-2-phenylindole (DAPI) (1:100 dilution; Biossci Biotechnology, Wuhan, China). The sections are examined with a Zeiss LSM 710 laser scanning confocal microscope (Carl Zeiss Meditec, Oberkochen, Germany) under excitation wavelengths of 405 nm for DAPI, 488 nm for Alexa Fluor 488, and 594 nm for Alexa Fluor 594.

VIP Administration in Animals In Vivo

Male Sprague–Dawley rats from the Experiment Animal Center of Tongji Medical College (220–280 g) were used for the experiments. All animals were raised in a 12-hour light/dark cycle and were given free access to food and water. The animals were maintained in adherence to the ARVO Statement for the Use of Animals in Ophthalmic and Vision Research and under protocols approved by the Institutional Animal Care and Use Committees of Huazhong University of Science and Technology (2015-K-023).

VIP (HSDAVFTDNYTRLRKQMAVKKYLNSILN) and VIP with N-terminal fluorescein isothiocyanate (FITC)-Acp were synthesized with purities of 98% (Sangon Biotech, Shanghai, China). These peptides were administered locally by eye drops. To instill the drops, we opened the eyelids of each rat and instilled one drop of drug into the central cornea, with blinking prevented, at intervals of 15 seconds. The right eye of each rat received a 10-µM VIP drop (Yick-Vic Chemicals & Pharmaceuticals, Hong Kong, China), and the left eye of each rat received a 50-µM VIP drop. Eye drops were administered once every 30 minutes for 6 continuous hours. Six, 12, and 24 hours after the start of the VIP eye drop administration, rats were sacrificed for eye collection. Another group of animals received water eye drops once every 30 minutes for 6 continuous hours as controls.

Using the same method, we also locally administered VIP–FITC (10 µM) eye drops to rats once every 30 minutes for 6 continuous hours to evaluate whether VIP can penetrate the cornea and reach the anterior chamber, iris, TM, SC, and retina.

SC Measurements Ex Vivo

SC was marked using HE and immunohistochemical (CD31) staining, as described above. The SC area were measured using ImageJ software (National Institutes of Health, Bethesda, MD, USA) by three independent and masked analyzers. Brightness and contrast were subjectively defined in order to maximize the visualization of SC. The area was drawn freehand based on the outline of SC. IOP was measured using a Tono-Pen XL tonometer (Reichert Technologies, Depew, NY, USA).

Safety of Local Application of VIP to the Eyes In Vivo

Rats received local water or VIP eye drops once a day for 2 weeks. To test the integrity of the corneal epithelium, 0.5% fluorescein sodium solution (10 µL) was instilled in the conjunctival sac of the rats. After 30 seconds, the excess fluorescein was rinsed with 0.9% NaCl solution. Cobalt blue light of a slit-lamp microscope (SL-D7; Topcon, Tokyo, Japan) with a digital camera was used for image acquisition. The lens transparency was also recorded using this imaging system with normal light. To test the viability of the corneal endothelium, dual staining of Alizarin Red S (to identify cell borders) and trypan blue (to identify cells with damaged plasma membranes) was applied. Each cornea was placed with the endothelium side up, and 0.25% trypan blue was dropped onto the endothelium for 90 seconds. After that, the trypan blue was rinsed with 0.9% NaCl solution, and 0.2% Alizarin Red S (pH 4.2) was dropped onto the endothelium for 120 seconds, followed by rinsing with 0.9% NaCl solution.[38] Cell viability was estimated by measuring the area of 50 contiguous endothelial cells in each visual field.[39] To count the retinal ganglion cells in both the VIP and water-treated groups, Brn-3a, a retinal ganglion cell marker, was labeled by immunofluorescence with a specific Brn-3a primary antibody (SC-8429, 1:200 dilution; Santa Cruz Biotechnology).

LRRK2 Immunofluorescence in SC of Rats Ex Vivo

In addition, LRRK2 immunofluorescence was performed in the SC of rats. The staining method was carried out as mentioned above. Primary antibody (ab133476, 1:50 dilution; Abcam) and Alexa Fluor 594-conjugated donkey anti-rabbit secondary antibody (1:200 dilution; Thermo Fisher Scientific) were used to evaluate local LRRK2 expression in SC in different groups.

Determination of Sp1 and LRRK2 Levels After Administration of VIP in HUVECs In Vitro

HUVECs were maintained in Dulbecco's Modified Eagle's Medium supplemented with Gibco 10% fetal bovine serum (Thermo Fisher Scientific), penicillin (100 U/mL)/streptomycin (100 µg/mL), and 2-mM L-glutamine at 37.8°C in 5% CO_2. A previous study identified potential

transcription factors of LRRK2 and noted that Sp1 can regulate the promoter activity and gene expression of LRRK2. Based on this, we tested the changes in the RNA expression of Sp1, GATA1/2, AP-1, HNF-3α, and NF-AT1[40] after the administration of VIP (1, 10, or 50 µM) for 6 hours in HUVECs. HUVECs were isolated with TRIzol Reagent (Thermo Fisher Scientific), and total RNA was collected and quantified. The collected RNA was reverse-transcribed into cDNA using a cDNA synthesis kit (Thermo Fisher Scientific) and amplified by quantitative polymerase chain reaction (qPCR) using the KAPASYBR FAST qPCR Master Mix (2X) Kit (KAPA Biosystems, Cape Town, South Africa) and an Applied Biosystems real-time PCR system (Thermo Fisher Scientific). Relative gene expression levels were normalized to the level of glyceraldehyde 3-phosphate dehydrogenase (GAPDH). The sequences for each primer are as follows:

- GAPDH—sense, 5′-AGCCACATCGCTCAGACAC-3′; antisense, 5′-GCCCAATACGACCAAATCC-3′
- Sp1—sense, 5′-TTGGGTACTTCAGGAATCCAGG-3′; antisense, 5′-CTGGGCTGTTTTCTCCTTCCT
- GATA1—sense, 5′-GCACCAACTGCCAGACGACC-3′; antisense, 5′-CAGATGCCTTGCGGTTTCGA-3′
- GATA2—sense, 5′-TGAAGAAGGAAGGGATCCAG-3′; antisense, 5′-TGGAGAGCTCCTCGAAACAT-3′)
- AP-1—sense, 5′-GAGTCTCAGGAGCGGATCAA-3′; antisense, 5′-TGAGTTGGCACCCACTGTTA-3′
- HNF-3α—sense, 5′-CTCTAGGCAGCGCCTCGGTGA-3′; antisense, 5′-CAGCATGGCTATGCCAGACAAACCC-3′
- NF-AT1—sense, 5′-CCTCGCCAATAATGTCACCT-3′; antisense, 5′-CGCGTGTTCTTTCTTCCAAT-3′

The expression of LRRK2 RNA in different intervention groups was examined in the same way: sense, 5′-ATGATGACAGCACAGCTAGGA-3′; antisense,5′-AAACGGTCAAGCAAGATTGTA-3′.

For western blotting of Sp1 and LRRK2, after being treated with VIP (1, 10, or 50 µM) for 6 hours HUVECs were lysed with radioimmunoprecipitation assay lysis buffer (P0013K; Beyotime Biotech, Beijing, China) on ice for 10 minutes and centrifuged at 16,000×g for 10 minutes. The supernatant was collected and loaded for western blotting analysis using antibodies specific for Sp1 (ab124804; Abcam) and LRRK2 (ab133476; Abcam) at 1:5000 dilutions. Moreover, we also extracted nuclear and cytoplasmic proteins using a nuclear protein extraction kit (Beyotime Biotech) to determine Sp1 expression in different subcellular locations. The cytoplasmic and nuclear components were subjected to western blotting.

In addition, we also performed immunofluorescence for Sp1 in HUVECs on coverslips with a primary antibody specific for Sp1 (ab124804, 1:200 dilution; Abcam) and secondary antibody (Alexa Fluor 594-conjugated donkey anti-rabbit), and DAPI (1:100 dilution; Biossci Biotech) to determine the expression of Sp1 in the nuclei.

Determination of Sp1 and LRRK2 Levels After Administration of Sp1/LRRK2 Inhibitor and VIP in HUVECs In Vitro

HUVECs were first treated with the Sp1 inhibitor plicamycin (50 µM) (ab142723; Abcam) for 24 hours or the LRRK2 inhibitor, LRRK2-IN-1 (3 µM) (S7584; Selleck Chemicals, Houston, TX, USA) for 120 minutes. The medium was then changed, and the HUVECs were treated with VIP (1, 10, or 50 µM)) for another 6 hours. After this, the HUVECs were collected and used for western blotting analysis to determine the protein expression levels of Sp1 and LRRK2.

Determination of the F-/G-Actin Ratio in HUVECs In Vitro

For cell experiments, VIP (1, 10, or 50 µM) was added to the culture medium for 6 hours and changes in the F-/G-actin ratio were examined using immunofluorescence and western blotting. We also tested the F-/G-actin ratio after HUVECs were treated with the LRRK2 inhibitor LRRK2-IN-1. To do this, we first incubated HUVECs with culture medium containing LRRK2-IN-1 (3 µM) for 120 minutes[41] and then exchanged the culture medium with VIP (1, 10, or 50 µM) for another 6 hours. For immunofluorescence in HUVECs on coverslips, F-actin was labeled with Alexa Fluor 594 phalloidin (1:1000 dilution; ab112127, Abcam), and G-actin was labeled with Alexa Fluor 488 deoxyribonuclease I (300 nM) for 1 hour at room temperature. For western blotting, radioimmunoprecipitation assay lysis buffer (P0013K; Beyotime Biotech) was employed to lyse HUVECs from the control and VIP (1, 10, and 50 µM) groups on ice for 10 minutes, followed by centrifugation at 15,000×g for 30 minutes. Soluble actin (G-actin) was collected in the supernatant. The insoluble F-actin in the pellet was resuspended in lysis buffer with an equal volume of buffer 2 (1.5-mM guanidine hydrochloride, 1-mM sodium acetate, 1-mM $CaCl_2$, 1-mM adenosine triphosphate, and 20-mM Tris-HCl; pH 7.5) and incubated on ice for 1 hour, with gentle mixing every 15 minutes, to convert F-actin into soluble G-actin. The samples were then centrifuged at 15,000×g for 30 minutes, and F-actin was collected in the supernatant.[42] Samples from the supernatant (G-actin) and pellet (F-actin) fractions were analyzed by western blotting using an Abcam antibody specific for actin (ab179467, 1:5000 dilution).

Determination of F-/G-Actin Ratio in the SC of Rat Eyes Ex Vivo

Water, VIP (50 µM), and VIP (50 µM) + LRRK2-IN-1 (10 µM) were locally applied to the rat eyes. For the groups treated with water or VIP only, water or VIP eye drops were administered once every 30 minutes for 6 hours. For the group treated with VIP + LRRK2-IN-1, the LRRK2-IN-1 was applied once every 15 minutes for 2 hours before VIP was applied (once every 30 minutes for 6 hours). After this, the rats were sacrificed and the eyes were collected. For immunofluorescence in SC of rat eyes, F-actin was labeled with Alexa Fluor 594 phalloidin (1:1000 dilution), and G-actin was labeled with Alexa Fluor 488 deoxyribonuclease I (300 nM) for 1 hour at room temperature. Furthermore, the SC area was also measured in each group.

Data Analysis

Statistical analyses were performed with two-tailed paired/unpaired t-tests and ordinary one-way ANOVA with Dunnett's multiple comparison test using GraphPad Prism 6.0 (GraphPad Software, San Diego, CA, USA). A level of 5% was considered significant.

Investigative Ophthalmology & Visual Science

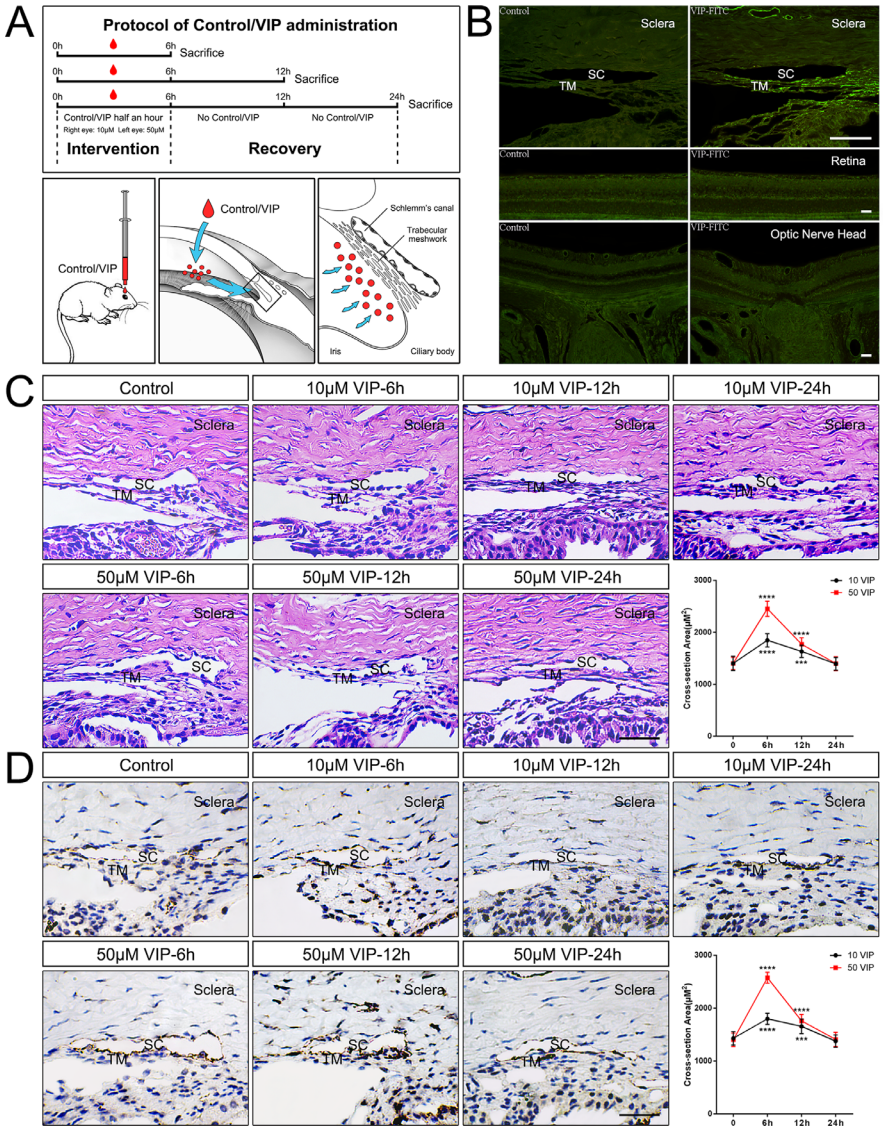

Figure 2. Effect of local VIP application on SC lumen size. (**A**) Protocol of VIP administration and schematic diagram of VIP distribution via the cornea. (**B**) Representative distribution of VIP–FITC (*green signal*) in the anterior segment (iris, trabecular meshwork, and SC), but not in the posterior segment (retina and optic nerve head). (**C**) Representative HE staining of the SC lumen and (**D**) immunohistochemical (CD31) staining of SC lumen. The SC lumen size increased significantly 6 hours and 12 hours after the start of local VIP application and returned to baseline values 24 hours after the start of local VIP application (each group n = 4). All groups were compared with the control. $^{***}P < 0.001$, $^{****}P < 0.0001$. *Scale bars*: 50 μm.

Results

Distribution of VIP and VPAC2 in the Region Surrounding Human SC

To confirm the location of SC in human eyes, serial slices were examined using HE staining and immunohistochemical (CD31) staining; CD31 is a biomarker for SC and could be used to locate SC[37,43] (Figs. 1B–1D). We found that SC was a thin, lucent space located at the corneoscleral junction in the iridocorneal angle area. To explore the distribution of VIP and VPAC2 receptor in the region surrounding SC, double immunofluorescence staining was performed; co-staining of VIP and VPAC2 has been observed in the area surrounding the lumen of human SC, as well as in human TM tissue (Figs. 1E–1L).

Local VIP Application Increases the Lumen Size of SC of Rats In Vivo

As shown in Figure 2B, after the local application of drops containing VIP with N-terminal FITC-Acp to rat eyes, a significant FITC fluorescence signal was observed in TM and SC areas. In contrast, no fluorescence signal was observed in TM and SC areas in the group that received local application of water eye drops (the control group). In the retina, no fluorescence signals were observed in the group that received eye drops containing VIP with N-terminal FITC-Acp (the treated group) or the group that received water eye drops (the control group). Both 10-μM and 50-μM VIP induced an increase in the lumen size of SC 6 hours and 12 hours after the start of local VIP drop application compared with the SC lumen size before local VIP drop application. However,

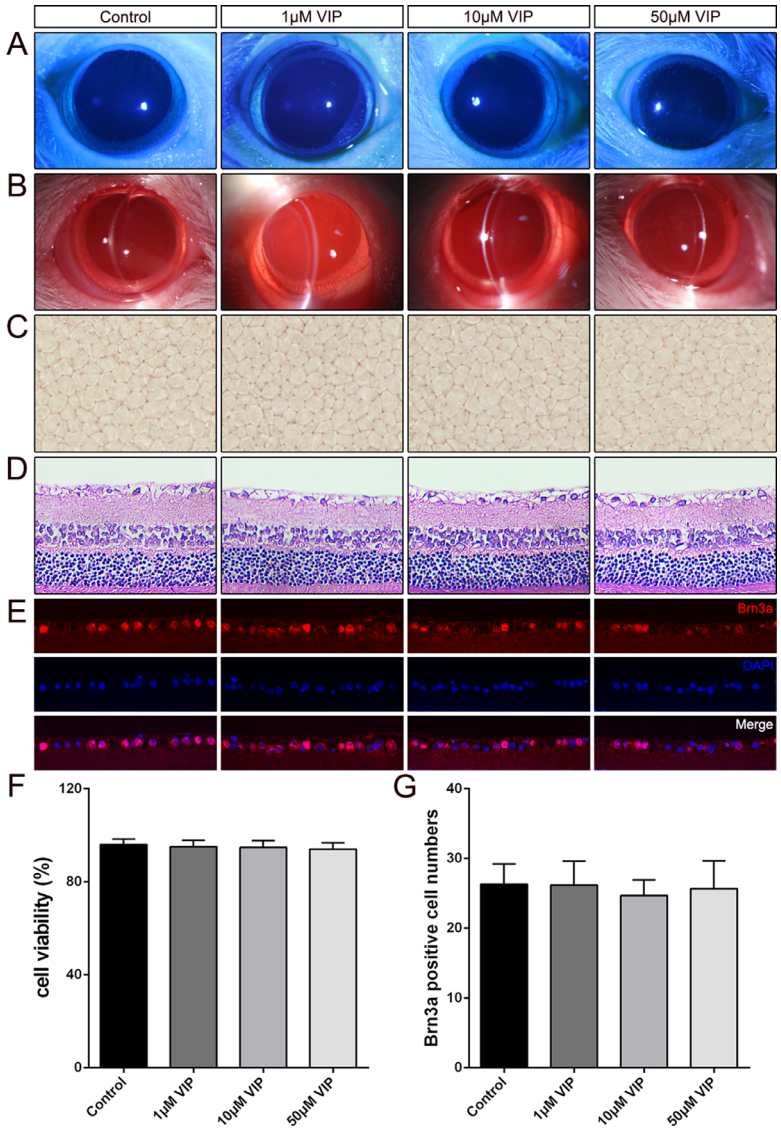

Figure 3. The safety of local VIP application in vivo. (**A**) Corneal fluorescence staining images were examined by cobalt blue light and showed no significant epithelium damage in the VIP groups. (**B**) Slit-lamp examination showed no significant lens opacity in the VIP groups. (**C**, **F**) Corneal flat-mounts stained with trypan blue and Alizarin Red S showed no significant changes in endothelium cell density or hexagonality in the VIP groups (each group n = 4). (**D**) HE staining of the retina in the VIP groups. (**E**, **G**) Immunofluorescence staining for Brn3a (*red*) and DAPI (*blue*) in retinal ganglion cells showed no significant decrease in the retinal ganglion cell number in the VIP groups (each group n = 6). All groups were compared with the control.

24 hours after the start of local VIP drop application, the SC lumen returned to the size they were before VIP application (the baseline size) (Figs. 2C, 2D). In the 50-μM VIP-treated group, IOP decreased significantly 6 hours after the start of local VIP drop application and returned to baseline 12 hours after the start of local VIP drop application. In the 10-μM VIP-treated group, no significant IOP reduction was observed after local VIP drop application (Supplementary Fig. S1). And controls for immunohistochemistry of human and rat tissue were shown in Supplementary Figure S2.

Safety of the Local Application of VIP in Rats In Vivo

After the local application of VIP (once a day for 2 weeks), there were no significant changes in the corneal epithelium or endothelium or in lens transparency compared with the control group. No significant corneal epithelium or endothelium damage and no significant lens opacity were observed (Figs. 3A–3C). Furthermore, there was no significant decrease in the retinal ganglion cell number after the local application of VIP (Figs. 3E, 3G).

Local VIP Application Upregulates LRRK2 Expression in Rats In Vivo and in HUVECs In Vitro

Using immunofluorescence staining to explore the expression of LRRK2 in SC endothelial cells in rat eyes, we found that 10-μM and 50-μM VIP upregulated the LRRK2 expression 6 hours after the start of local VIP drop application.

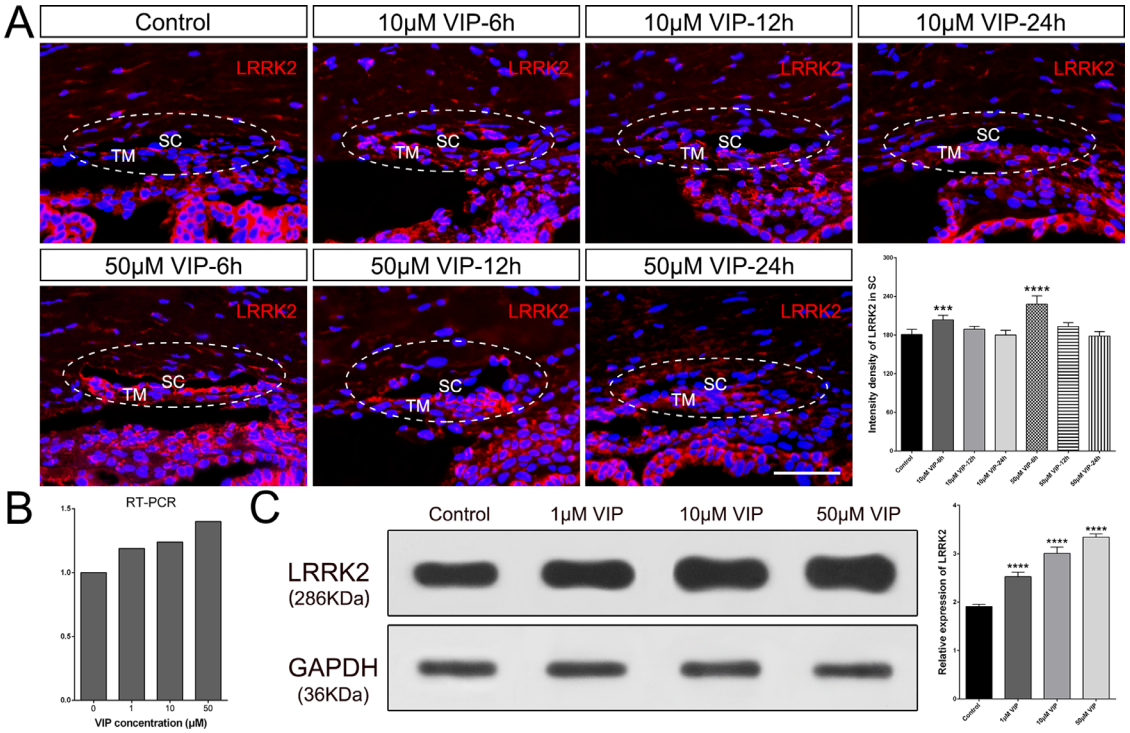

Figure 4. Immunofluorescence staining for LRRK2 in SC endothelial cells stimulated with VIP in vivo and the mRNA and protein expression of LRRK2 in HUVECs stimulated with VIP in vitro. (**A**) Representative immunofluorescence staining (*red*) for LRRK2 in SC endothelium cells. The immunofluorescence optical density of LRRK2 surrounding the SC endothelium increased significantly 6 hours after the start of local VIP application and returned to baseline values 12 hours after the start of local VIP application (each group n = 5). (**B**) The results of qPCR for LRRK2 in HUVECs upon VIP stimulation and (**C**) representative western blots of LRRK2 in HUVECs upon VIP stimulation. VIP increased the mRNA and protein expression levels of LRRK2 in HUVECs. All groups were compared with the control. $^{***}P < 0.001$, $^{****}P < 0.0001$. *Scale bars*: 50 μm.

Then, 12 hours later, the expression of LRRK2 surrounding SC returned to the pre-intervention (baseline) levels (Fig. 4A). The recovery of LRRK2 (within 12 hours) occurred before the recovery of the SC lumen (within 24 hours), indicating that the recovery of LRRK2 and the SC lumen occurred in sequence. LRRK2 returned to baseline first and then induced the recovery of the SC lumen via its regulatory effect on the actin cytoskeleton. Consistent with the aforementioned changes in LRRK2 expression induced by VIP in vivo, the mRNA and protein expression levels of LRRK2 also increased after HUVECs were treated with VIP (1, 10, or 50 μM) (Figs. 4B, 4C).

VIP Promotes the mRNA and Protein Expression of Sp1 in HUVECs In Vitro

A previous study identified potential transcription factors of LRRK2 and noted that Sp1 can regulate the promoter activity and gene expression of *LRRK2*.[40] The mRNA and protein expression levels of Sp1 showed the same trend as the expression levels of LRRK2 in this study; VIP (1, 10, or 50 μM) promoted the mRNA and protein expression levels of Sp1 in HUVECs (Figs. 5A, 5D). Furthermore, we observed that after treatment with VIP (1, 10, or 50 μM), the protein level of Sp1 in the cytoplasm remained relatively unchanged, whereas the protein level of Sp1 in the nucleus increased significantly (Figs. 5B, 5C). This increase in Sp1 in the nucleus induced by VIP (1, 10, or 50 μM) was also confirmed by immunofluorescence staining (Fig. 5E). These findings suggest that VIP was able to upregulate the expression of LRRK2 by promoting and recruiting Sp1 to the nucleus.

Effect of Sp1 and LRRK2 Inhibitor on the Protein Expression Levels of Sp1 and LRRK2 in HUVECs In Vitro

The Sp1 inhibitor (plicamycin) inhibited the expression of Sp1 by targeting DNA and RNA polymerase and DNA binding.[44] We observed that, compared with the group not treated with plicamycin, the plicamycin-treated group exhibited a significant decrease in the protein expression level of Sp1. In addition, upon plicamycin application, the protein expression level of LRRK2 also decreased significantly (Fig. 6A). LRRK2-IN-1 is an LRRK2 inhibitor that inhibits only the biological activity of LRRK2,[45,46] and our study results indicate that the application of LRRK2-IN-1 did not have an effect on the protein expression of LRRK2 and Sp1 induced by VIP. Thus, the application of LRRK2-IN-1 did not influence the effect of VIP on Sp1 and LRRK2 expression (Fig. 6B).

In HUVECs, VIP Decreases the F-/G-Actin Ratio and LRRK2-IN-1 Eliminates This Effect of VIP In Vitro

Using immunofluorescence staining and western blotting, we found that after the application of VIP (1, 10, or 50 μM)

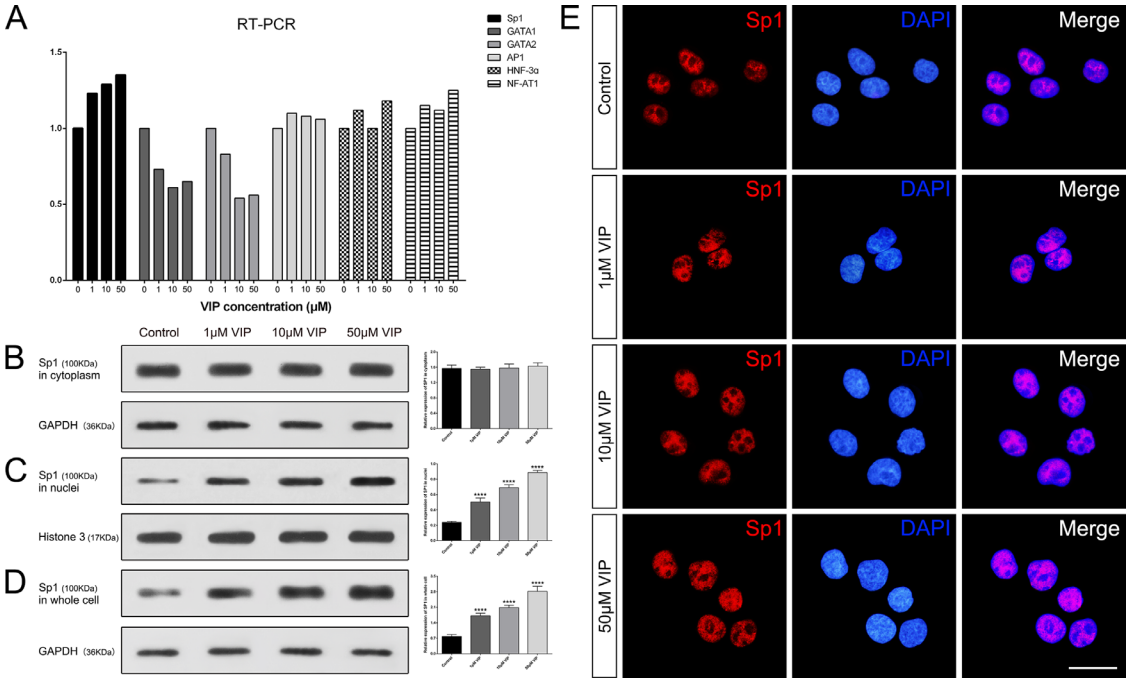

Figure 5. The mRNA and protein expression of Sp1 in HUVECs stimulated with VIP. (**A**) The results of qPCR for Sp1 in HUVECs stimulated with VIP. Representative western blots of Sp1 in the cytoplasm (**B**), nuclei (**C**), and whole cell (**D**). The protein level of Sp1 in the cytoplasm remained relatively unchanged, whereas the protein level of Sp1 in the nuclei showed a significant increase in HUVECs stimulated with VIP. (**E**) Representative immunofluorescence staining for Sp1 (*red*) and DAPI (*blue*) in the nuclei of HUVECs. Nuclear Sp1 increased in HUVECs stimulated with VIP. All groups were compared with the control. $^{****}P < 0.0001$. *Scale bars*: 50 μm.

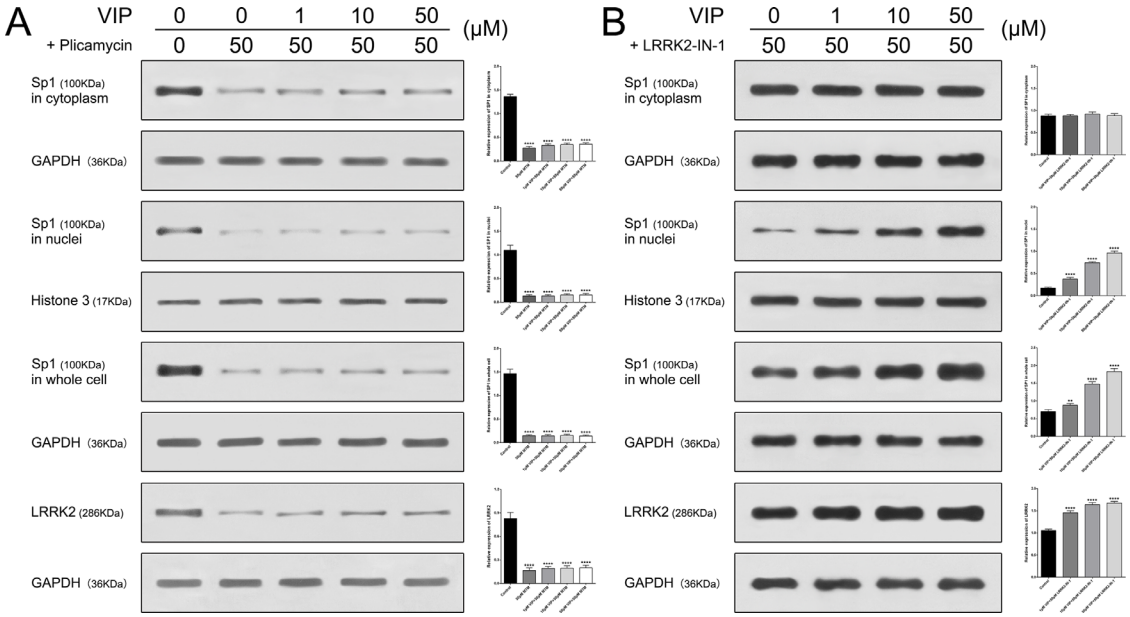

Figure 6. Western blotting for Sp1 and LRRK2 in HUVECs stimulated with VIP + Sp1/LRRK2 inhibitor. (**A**) Representative western blots of Sp1 and LRRK2 in HUVECs treated with the VIP + Sp1 inhibitor plicamycin. Plicamycin inhibited the expression of Sp1 by targeting DNA and RNA polymerase and DNA binding. The application of plicamycin decreased the protein expression of both Sp1 and LRRK2. (**B**) Representative western blots of Sp1 and LRRK2 in HUVECs treated with VIP + LRRK2 inhibitor (LRRK2-IN-1). LRRK2-IN-1 inhibited only the biological activity of LRRK2 and thus had no influence on the protein expression of Sp1 and LRRK2 induced by VIP. All groups were compared with the control. $^{**}P < 0.01$, $^{****}P < 0.0001$.

Investigative Ophthalmology & Visual Science

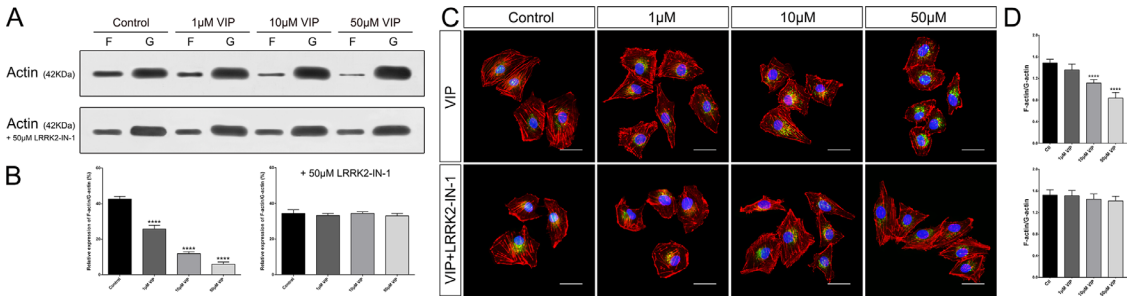

Figure 7. Western blotting and immunofluorescence staining of F-actin and G-actin in HUVECs stimulated with VIP and with VIP+LRRK2-IN-1. Representative (**A**) western blots and (**C**) immunofluorescence staining (*red* for F-actin and *green* for G-actin) for F-actin and G-actin in HUVECs. (**B**, **D**) VIP induced a decrease in the F-/G-actin ratio, and this effect was abolished by the application of LRRK2-IN-1. All groups were compared with the control. $^{****}P < 0.0001$. *Scale bars*: 50 μm.

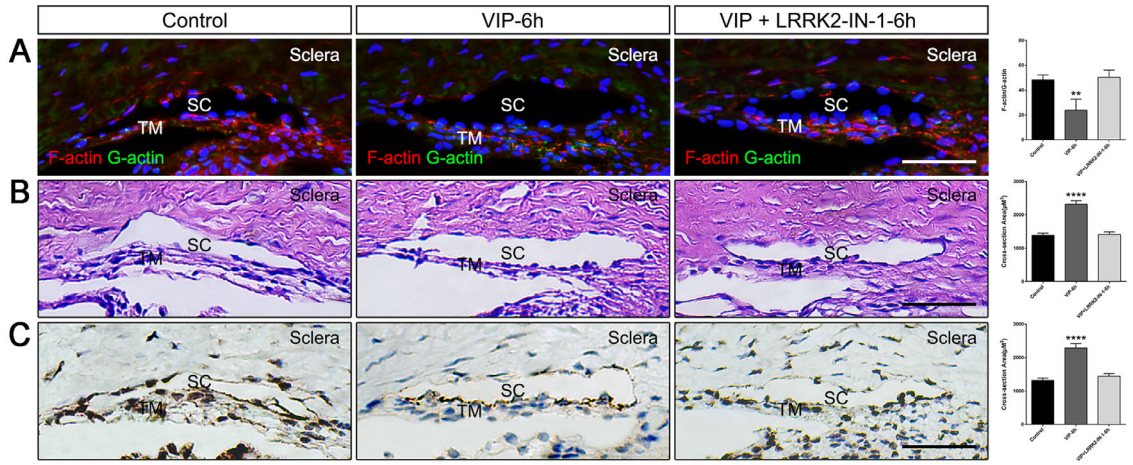

Figure 8. Immunofluorescence staining for F-actin and G-actin in SC endothelial cells stimulated with VIP and with VIP + LRRK2-IN-1. (**A**) Representative immunofluorescence staining of F-actin (*red*), G-actin (*green*), and DAPI (*blue*) in the SC endothelium. VIP decreased the F-/G-actin ratio in the SC endothelium, whereas the application of LRRK2-IN-1 eliminated this effect. (**B**) Representative HE staining of the SC lumen, and (**C**) immunohistochemical (CD31) staining of the SC lumen. VIP expanded the SC lumen, whereas the application of LRRK2-IN-1 abolished this effect. All groups were compared with the control (each group n = 4). $^{**}P < 0.01$, $^{****}P < 0.0001$. *Scale bars*: 50 μm.

for 6 hours, the F-/G-actin ratio for HUVECs decreased significantly. Compared with the control group (no VIP), the cells in the 50-μM VIP group became rounded in shape. However, the application of the LRRK2 inhibitor LRRK2-IN-1 abolished this effect of VIP on the F-/G-actin ratio and cell shape (the F-/G-actin ratio and cell shape remained relatively unchanged with the application of LRRK2-IN-1) (Fig. 7).

LRRK2-IN-1 Eliminates the Change in the F-/G-Actin Ratio Induced by VIP in Rats In Vivo

We observed that compared with that in the control (water-treated) group, the fluorescence signal of G-actin (green) surrounding SC increased and that of F-actin (red) decreased, leading to significant changes in the F-/G-actin ratio after VIP eye drop treatment. In contrast, in the group treated with VIP + LRRK2-IN-1, the fluorescence signals of G-actin and F-actin remained relatively unchanged after drug intervention; thus, the F-/G-actin ratio was consistent with that in the control (water-treated) group (Fig. 8A). In addition, LRRK2-IN-1 eliminated the expansion of the SC lumen by VIP, whereas the group treated only with VIP had a significantly larger SC lumen than the water-treated control group (Figs. 8B, 8C).

Discussion

Elevated IOP is the main risk factor for glaucoma, and this pathological change can be attribute to the increase in the aqueous humor outflow resistance, which is closely correlated with the cytoskeleton of the SC endothelium.[3,4,27] In our previous study, we reported the effect of VIP on the morphology and cytoskeleton of the SC endothelium and IOP.[27] However, the molecular mechanism of the effect of VIP on the cytoskeleton of endothelial cell is still not completely clear. In this present study, we found that VIP increased the expression level of Sp1 and induced its migration from the cytoplasm into the nucleus. After the recruitment of Sp1 to the nucleus, it can further upregulate the expression level of LRRK2. Next, the effect of LRRK2 on the cytoskeleton (F-actin and G-actin) was examined. With the increase in LRRK2, the F-/G-actin ratio decreased significantly. After the application of LRRK2 inhibitor (LRRK2-IN-1), the phosphorylation of LRRK2 was inhibited,[45,46] which resulted in the inactivation of the biological activity of

LRRK2. The F-/G-actin ratio can remain relatively unchanged upon VIP treatment, indicating that the effect of VIP on the cytoskeleton (F-actin and G-actin) was abolished by the LRRK2 inhibitor and that LRRK2 plays an important role in the regulation of the F-actin and G-actin balance.

The spatial structure of the cytoskeleton network is important and necessary for transmitting compressive and tensile stresses and for sensing the mechanical microenvironment.[47] Previous studies have indicated that the stiffness of SC endothelial cells is determined by the cell cytoskeleton and contributes to aqueous humor outflow resistance.[13–21,24,25,48] Stiffer SC endothelial cells would deform less under a transcellular pressure drop, thus inhibiting pore formation and decreasing the aqueous humor outflow facility.[20,49] Using drug intervention, previous studies have also confirmed the role of SC endothelial cell stiffness in aqueous humor outflow resistance regulation.[50,51] Thus, the increased stiffness of SC endothelial cells could be a major reason for the elevation of IOP and the pathogenesis of glaucoma. In this present study, we found that, in the human SC endothelium, VIP and VPAC2 were co-expressed, indicating that VIP and its receptor exist around SC, providing SC with the structural foundation for VIP regulation. In our animal experiments, we confirmed the ability of VIP to expand the SC lumen and that this effect was achieved by the regulatory effect of VIP on the cytoskeleton (the F-/G-actin ratio). When VIP downregulated the F-/G-actin ratio, the stiffness of the SC endothelium was also reduced,[24,25] leading to an increase in SC lumen size and a decrease in the aqueous humor outflow resistance.[52,53] Also, our present study has shown that, after topical VIP application, the expanded SC lumen recovered to its pretreatment size within 24 hours, indicating that the ability of VIP to expand the SC lumen has a time limit.

The *LRRK2* gene encodes a large, multidomain protein that has 2527 amino acids and belongs to the ROCO protein superfamily. The LRRK2 protein contains a couple of distinctive structural domains, including a ROC/GTPase domain and a kinase domain. In between these two domains is located a C-terminal of Ras complex domain.[28,29] LRRK2 has been reported to play a critical role in actin cytoskeleton remodeling and to be a direct or indirect regulator of actin polymerization.[30–32] Regarding the mechanisms by which LRRK2 regulates the actin cytoskeleton, recent studies have reported that LRRK2 can interact with the small GTPases CDC42 and Rac1, which are key regulators of actin polymerization[31,33] and can regulate the phosphorylation of the actin-binding proteins ezrin, radixin, and moesin, which are crucial for the anchorage of actin filaments to the cell membrane.[34] In addition, LRRK2 can also interact with actin isoforms and with proteins that regulate actin stability and maintenance (e.g., capping proteins, tropomyosins, actin motor proteins) to further regulate the balance between stabilization and destabilization of the F-actin architecture.[32] A previous LRRK2 knockdown experiment in cells also confirmed that LRRK2 may be a central mediator of the actin cytoskeleton network.[54] In this study, we applied LRRK2 inhibitor to HUVECs and found that the LRRK2 inhibitor eliminated the effect of VIP on the actin cytoskeleton, although the expression levels of Sp1 and LRRK2 were still upregulated by VIP, indicating that LRRK2 is an important mediator of actin cytoskeleton remodeling induced by VIP.

According to the transcription factor binding sites of the *LRRK2* gene, a previous study identified several putative transcription factors for LRRK2, including Sp1, GATA1/2, AP-1, HNF-3α, and NF-AT1.[40] In this study, we evaluated the changes in RNA expression after the application of VIP to HUVECs and found that Sp1 showed the most significant positive changes, indicating that VIP can positively regulate the RNA expression of Sp1. In addition, a previous study also confirmed that Sp1 is able to regulate the promoter activity and gene expression of *LRRK2*.[40] Consistent with the PCR results, our western-blotting results showed that, after the application of VIP to HUVECs, the protein level of Sp1 increased, Sp1 translocated to the nucleus, and there was a simultaneous increase in the protein level of LRRK2. When the Sp1 inhibitor plicamycin, which can bind to GC-rich sequences with high affinity and act as a site-specific inhibitor of Sp1,[55,56] was applied, the protein level of Sp1 decreased, with a simultaneous decrease in the protein level of LRRK2. The trends of changes in Sp1 and LRRK2 were identical under different drug interventions (VIP and plicamycin). This study result is also consistent with a previous study that indicated that Sp1 signaling is important for the regulation of *LRRK2* gene expression.[40] Sp1 is a classic transcription factor involved in various molecular pathways and can bind to GC-boxes and GT/CACC-boxes. Its binding sequence is (G/T)GGGCGG(G/A)(G/A)(C/T),[35,36] which also appears in the LRRK2 promoter; thus, Sp1 can bind to the *LRRK2* promotor and upregulate the expression of LRRK2.[40]

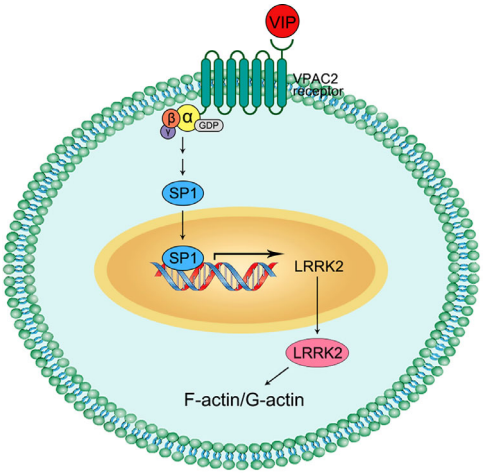

Figure 9. Schematic diagram of the effect of VIP on the cytoskeleton. VIP induced an increase in the expression of transcription factor Sp1 and then recruited Sp1 into the nuclei. After that, the migration of Sp1 to nuclei upregulated the expression of LRRK2, which would further change the ratio of F-actin and G-actin.

A major limitation of this study was that we performed experiments on HUVECs rather than primary SC cells. It is not clear whether our HUVEC experiment results could also be observed in primary SC cells; thus, further studies on primary SC cells would be necessary.

In conclusion, the application of VIP induces an increase in the expression of the transcription factor Sp1 and then recruits Sp1 to the nucleus. After that, the translocation of Sp1 to the nucleus upregulates the expression of LRRK2, which further changes the F-/G-actin ratio and regulates the balance between stabilization and destabilization of the F-actin architecture (Fig. 9).

Investigative Ophthalmology & Visual Science

Acknowledgments

Supported by grants from the National Natural Science Foundation of China (81770921, 81800821, and 81700834).

Disclosure: **X. Yan,** None; **M. Li,** None; **Z. Luo,** None; **Y. Zhao,** None; **H. Zhang,** None; **L. Chen,** None

References

1. Flaxman SR, Bourne RRA, Resnikoff S, et al. Global causes of blindness and distance vision impairment 1990-2020: a systematic review and meta-analysis. *Lancet Glob Health*. 2017;5:e1221–e1234.
2. Tham YC, Li X, Wong TY, Quigley HA, Aung T, Cheng CY. Global prevalence of glaucoma and projections of glaucoma burden through 2040: a systematic review and meta-analysis. *Ophthalmology*. 2014;121:2081–2090.
3. Gordon MO, Beiser JA, Brandt JD, et al. The Ocular Hypertension Treatment Study: baseline factors that predict the onset of primary open-angle glaucoma. *Arch Ophthalmol*. 2002;120:714–720; discussion 829–830.
4. Topouzis F, Wilson MR, Harris A, et al. Risk factors for primary open-angle glaucoma and pseudoexfoliative glaucoma in the Thessaloniki eye study. *Am J Ophthalmol*. 2011;152:219–228.e1.
5. McDonnell F, Dismuke WM, Overby DR, Stamer WD. Pharmacological regulation of outflow resistance distal to Schlemm's canal. *Am J Physiol Cell Physiol*. 2018;315:C44–C51.
6. Alm A, Grierson I, Shields MB. Side effects associated with prostaglandin analog therapy. *Surv Ophthalmol*. 2008;53(suppl 1):S93–S105.
7. Schmidl D, Schmetterer L, Garhöfer G, Popa-Cherecheanu A. Pharmacotherapy of glaucoma. *J Ocul Pharmacol Ther*. 2015;31:63–77.
8. Johnson DH. Human trabecular meshwork cell survival is dependent on perfusion rate. *Invest Ophthalmol Vis Sci*. 1996;37:1204–1208.
9. Kopczynski CC, Epstei DL. Emerging trabecular outflow drugs. *J Ocul Pharmacol Ther*. 2014;30:85–87.
10. Dismuke WM, Mbadugha CC, Ellis DZ. NO-induced regulation of human trabecular meshwork cell volume and aqueous humor outflow facility involve the BKCa ion channel. *Am J Physiol Cell Physiol*. 2008;294:C1378–C1386.
11. Harris A, Ward CL, Rowe-Rendleman CL, et al. Ocular hypotensive effect of ONO-9054, an EP3/FP receptor agonist: results of a randomized, placebo-controlled, dose escalation study. *J Glaucoma*. 2016;25:e826–e833.
12. Tanihara H, Inoue T, Yamamoto T, et al. Intra-ocular pressure-lowering effects of a Rho kinase inhibitor, ripasudil (K-115), over 24 hours in primary open-angle glaucoma and ocular hypertension: a randomized, open-label, crossover study. *Acta Ophthalmol*. 2015;93:e254–e260.
13. Kaufman PL, Bill A, Bárány EH. Effect of cytochalasin B on conventional drainage of aqueous humor in the cynomolgus monkey. *Exp Eye Res*. 1977;25(suppl):411–414.
14. Tian B, Kaufman PL, Volberg T, Gabelt BT, Geiger B. H-7 disrupts the actin cytoskeleton and increases outflow facility. *Arch Ophthalmol*. 1998;116:633–643.
15. Peterson JA, Tian B, Bershadsky AD, et al. Latrunculin-A increases outflow facility in the monkey. *Invest Ophthalmol Vis Sci*. 1999;40:931–941.
16. Peterson JA, Tian B, Geiger B, Kaufman PL. Effect of latrunculin-B on outflow facility in monkeys. *Exp Eye Res*. 2000;70:307–313.
17. Tian B, Geiger B, Epstein DL, Kaufman PL. Cytoskeletal involvement in the regulation of aqueous humor outflow. *Invest Ophthalmol Vis Sci*. 2000;41:619–623.
18. Tanna AP, Johnson M. Rho kinase inhibitors as a novel treatment for glaucoma and ocular hypertension. *Ophthalmology*. 2018;125:1741–1756.
19. Svedbergh B, Lütjen-Drecoll E, Ober M, Kaufman PL. Cytochalasin B-induced structural changes in the anterior ocular segment of the cynomolgus monkey. *Invest Ophthalmol Vis Sci*. 1978;17:718–734.
20. Zhou EH, Krishnan R, Stamer WD, et al. Mechanical responsiveness of the endothelial cell of Schlemm's canal: scope, variability and its potential role in controlling aqueous humour outflow. *J R Soc Interface*. 2012;9:1144–1155.
21. Overby DR, Zhou EH, Vargas-Pinto R, et al. Altered mechanobiology of Schlemm's canal endothelial cells in glaucoma. *Proc Natl Acad Sci USA*. 2014;111:13876–13881.
22. Inoue T, Tanihara H. Rho-associated kinase inhibitors: a novel glaucoma therapy. *Prog Retin Eye Res*. 2013;37:1–12.
23. Rao PV, Deng PF, Kumar J, Epstein DL. Modulation of aqueous humor outflow facility by the Rho kinase-specific inhibitor Y-27632. *Invest Ophthalmol Vis Sci*. 2001;42:1029–1037.
24. Warnock DG, Kusche-Vihrog K, Tarjus A, et al. Blood pressure and amiloride-sensitive sodium channels in vascular and renal cells. *Nat Rev Nephrol*. 2014;10:146–157.
25. Zhou N, Lee JJ, Stoll S, Ma B, Costa KD, Qiu H. Rho kinase regulates aortic vascular smooth muscle cell stiffness via actin/SRF/myocardin in hypertension. *Cell Physiol Biochem*. 2017;44:701–715.
26. Rao PV, Pattabiraman PP, Kopczynski C. Role of the Rho GTPase/Rho kinase signaling pathway in pathogenesis and treatment of glaucoma: bench to bedside research. *Exp Eye Res*. 2017;158:23–32.
27. Chen L, Li M, Luo Z, et al. VIP regulates morphology and F-actin distribution of Schlemm's canal in a chronic intraocular pressure hypertension model via the VPAC2 receptor. *Invest Ophthalmol Vis Sci*. 2018;59:2848–2860.
28. Mata IF, Wedemeyer WJ, Farrer MJ, Taylor JP, Gallo KA. LRRK2 in Parkinson's disease: protein domains and functional insights. *Trends Neurosci*. 2006;29:286–293.
29. Zimprich A, Bisku S, Leitner P, et al. Mutations in LRRK2 cause autosomal-dominant parkinsonism with pleomorphic pathology. *Neuron*. 2004;44:601–607.
30. Alegre-Abarrategui J, Christian H, Lufino MM, et al. LRRK2 regulates autophagic activity and localizes to specific membrane microdomains in a novel human genomic reporter cellular model. *Hum Mol Genet*. 2009;18:4022–4034.
31. Haebig K, Gloeckner CJ, Miralles MG, et al. ARHGEF7 (Beta-PIX) acts as guanine nucleotide exchange factor for leucine-rich repeat kinase 2. *PLoS One*. 2010;5:e13762.
32. Meixner A, Boldt K, Van Troys M, et al. A QUICK screen for Lrrk2 interaction partners–leucine-rich repeat kinase 2 is involved in actin cytoskeleton dynamics. *Mol Cell Proteomics*. 2011;10:M110.001172.
33. Chan D, Citro A, Cordy JM, Shen GC, Wolozin B. Rac1 protein rescues neurite retraction caused by G2019S leucine-rich repeat kinase 2 (LRRK2). *J Biol Chem*. 2011;286:16140–16149.
34. Parisiadou L, Xie C, Cho HJ, et al. Phosphorylation of ezrin/radixin/moesin proteins by LRRK2 promotes the rearrangement of actin cytoskeleton in neuronal morphogenesis. *J Neurosci*. 2009;29:13971–13980.
35. Briggs MR, Kadonaga JT, Bell SP, Tjian R. Purification and biochemical characterization of the promoter-specific transcription factor, Sp1. *Science*. 1986;234:47–52.
36. Giglioni B, Comi P, Ronchi A, Mantovani R, Ottolenghi S. The same nuclear proteins bind the proximal CACCC box of the human beta-globin promoter and a similar

Investigative Ophthalmology & Visual Science

sequence in the enhancer. *Biochem Biophys Res Commun*. 1989;164:149–155.

37. Ji P, Chen L, Gong J, et al. Co-expression of vasoactive intestinal peptide and protein gene product 9.5 surrounding the lumen of human Schlemm's canal. *Exp Eye Res*. 2018;170:1–7.
38. Kim JA, Ko JH, Ko AY, et al. TSG-6 protects corneal endothelium from transcorneal cryoinjury in rabbits. *Invest Ophthalmol Vis Sci*. 2014;55:4905–4912.
39. Lively GD, Jiang B, Hedberg-Buenz A, et al. Genetic dependence of central corneal thickness among inbred strains of mice. *Invest Ophthalmol Vis Sci*. 2010;51:160–171.
40. Wang J, Song W. Regulation of LRRK2 promoter activity and gene expression by Sp1. *Mol Brain*. 2016;9:33.
41. Zhang J, Deng X, Choi HG, Alessi DR, Gray NS. Characterization of TAE684 as a potent LRRK2 kinase inhibitor. *Bioorg Med Chem Lett*. 2012;22:1864–1869.
42. Zeidan A, Paylor B, Steinhoff KJ, et al. Actin cytoskeleton dynamics promotes leptin-induced vascular smooth muscle hypertrophy via RhoA/ROCK- and phosphatidylinositol 3-kinase/protein kinase B-dependent pathways. *J Pharmacol Exp Ther*. 2007;322:1110–1116.
43. Heimark RL, Kaochar S, Stamer WD. Human Schlemm's canal cells express the endothelial adherens proteins, VE-cadherin and PECAM-1. *Curr Eye Res*. 2002;25:299–308.
44. Jia Z, Gao Y, Wang L, et al. Combined treatment of pancreatic cancer with mithramycin A and tolfenamic acid promotes Sp1 degradation and synergistic antitumor activity. *Cancer Res*. 2010;70:1111–1119.
45. Deng X, Dzamko N, Prescott A, et al. Characterization of a selective inhibitor of the Parkinson's disease kinase LRRK2. *Nat Chem Biol*. 2011;7:203–205.
46. Weygant N, Qu D, Berry WL, et al. Small molecule kinase inhibitor LRRK2-IN-1 demonstrates potent activity against colorectal and pancreatic cancer through inhibition of doublecortin-like kinase 1. *Mol Cancer*. 2014;13:103.
47. Janmey PA, McCulloch CA. Cell mechanics: integrating cell responses to mechanical stimuli. *Annu Rev Biomed Eng*. 2007;9:1–34.
48. Stack T, Vahabikashi A, Johnson M, Scott E. Modulation of Schlemm's canal endothelial cell stiffness via latrunculin loaded block copolymer micelles. *J Biomed Mater Res A*. 2018;106:1771–1779.
49. Stamer WD, Braakman ST, Zhou EH, et al. Biomechanics of Schlemm's canal endothelium and intraocular pressure reduction. *Prog Retin Eye Res*. 2015;44:86–98.
50. Ethier CR, Read AT, Chan DW. Effects of latrunculin-B on outflow facility and trabecular meshwork structure in human eyes. *Invest Ophthalmol Vis Sci*. 2006;47:1991–1998.
51. Vargas-Pinto R, Gong H, Vahabikashi A, Johnson M. The effect of the endothelial cell cortex on atomic force microscopy measurements. *Biophys J*. 2013;105:300–309.
52. Allingham RR, de Kater AW, Ethier CR. Schlemm's canal and primary open angle glaucoma: correlation between Schlemm's canal dimensions and outflow facility. *Exp Eye Res*. 1996;62:101–109.
53. Li M, Zhao Y, Yan X, Zhang H. The relationship between the 24-hour fluctuations in Schlemm's canal and intraocular pressure: an observational study using high-frequency ultrasound biomicroscopy. *Curr Eye Res*. 2017;42:1389–1395.
54. Häbig K, Walter M, Poths S, Riess O, Bonin M. RNA interference of LRRK2-microarray expression analysis of a Parkinson's disease key player. *Neurogenetics*. 2008;9:83–94.
55. Ray R, Snyder RC, Thomas S, Koller CA, Miller DM. Mithramycin blocks protein binding and function of the SV40 early promoter. *J Clin Invest*. 1989;83:2003–2007.
56. Van Dyke MW, Dervan PB. Chromomycin, mithramycin, and olivomycin binding sites on heterogeneous deoxyribonucleic acid. Footprinting with (methidiumpropyl-EDTA) iron(II). *Biochemistry*. 1983;22:2373–2377.

Investigative Ophthalmology & Visual Science